



## Preparation, spectroscopic and thermal investigations on charge-transfer complexes formed in the reaction of ribavirin drug and various acceptors

Akmal S. Gaballa

Faculty of Specific Education, Zagazig University, Zagazig, Egypt

### ABSTRACT

Considerable attention has recently been given to the formation of stable charge-transfer complexes that result from the reaction between drugs and acceptors due to the significant physical and chemical properties of these complexes. Charge-transfer complexes formed between ribavirin (RV) as electron donor with different electron acceptors as iodine ( $I_2$ ), picric acid (HPA), chloranilic acid ( $H_2CA$ ), and 2,3-dichloro-5,6-dicyano-1,4-benzoquinone (DDQ) have been investigated in methanol at room temperature. Based on elemental analyses and IR spectra of the solid CT-complexes along with the photometric titration curves for the reactions, the stoichiometries of all complexes were found to be 1:2 molar ratio between RV and  $I_2$ , and 1:1 molar ratio between RV and acceptors (HPA,  $H_2CA$ , and DDQ). The infrared spectroscopic data indicate a charge transfer interaction associated with a proton migration from the acceptor to the donor followed by intramolecular hydrogen bonding in [(HRV)(PA)] and [(HRV)(HCA)] complexes. Another charge transfer interactions were observed in [(RV) $I$ ] $_3$ , and [(RV)(DDQ)] complexes. The characteristic physical constants ( $K_{CT}$ ,  $\mu$ ,  $\Delta G$ ,  $I_D$ ,  $f$ ,  $E_{CT}$ ) of the formed CT-complexes are shown to be strongly dependent on the type and structure of the electron acceptors.

**Key words:** Charge transfer; Ribavirin; Electron acceptors; UV-visible; IR; TGA spectrometry; Antibacterial activity.

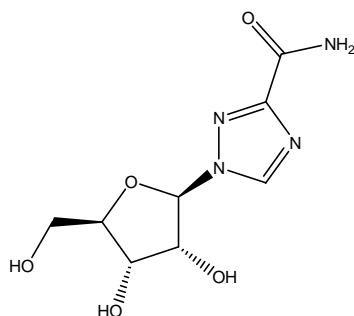
### INTRODUCTION

Charge-transfer (CT) complexes are formed by the interaction between electron donors and electron acceptors. CT complexation is an important phenomenon in biochemical and bioelectrochemical energy transfer process [1,2]. There is no sharp boundary between the coordination complexes and charge-transfer complexes. However, orbitally, in a CT-complex an electron may be transferred from a nonbonding orbital of the donor to an antibonding orbital of an acceptor. In a coordination complex, there is a donation of a lone pair of electrons from the donor to the vacant orbital of the acceptor. A large numbers of different complexes are stabilized by other bonding contributions [3].

In the past years, CT reaction has been widely studied. A large number of different types of drugs are easily determined by spectrophotometric techniques based on formation of stable CT complexes with electron acceptors [4]. The interactions of the charge-transfer complexes are well known in many chemical reactions such as addition, substitution, and condensation [5]. The molecular interactions between electron donors and acceptors are generally associated with the formation of intensely coloured charge transfer complexes, which absorb radiation in the visible region [6]. Electron donor-acceptor CT interactions are also important in the field of drug-receptor binding mechanism [7] as well as in many biological fields [8]. On the other hand, the CT-reactions of  $\pi$ -acceptors have successfully been utilized in pharmaceutical analysis [9].

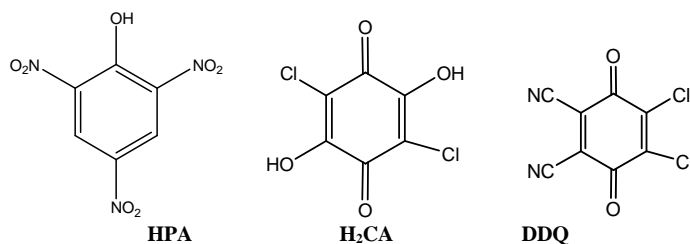
Ribavirin (RV, **I**) is a synthetic guanosine, in a class of antiviral medications called nucleoside analogues used to stop viral RNA synthesis and viral mRNA capping, thus, it is a nucleoside inhibitor [10] and used for the treatment of human respiratory virus and orally to treat hepatitis C in combination with interferon [11,12], now with

Sofosbuvir drug (Sovaldi) [13-15] and some other viral infections [16,17]. Ribavirin is a prodrug, which when metabolized resembles purine RNA nucleotides. In this form, it interferes with RNA metabolism required for viral replication [18,19]. It works by stopping the virus that causes hepatitis C from spreading inside the body. It is not known if treatment that includes ribavirin and another medication cures hepatitis C infection, prevents liver damage that may be caused by hepatitis C, or prevents the spread of hepatitis C to other people.



I. Structure of Ribavirin (RV)

To continue our interest in studying the synthesis and spectroscopic characterization of various CT-complexes in order to understand the nature of their CT-interaction [20-25], we have investigated the CT interaction of the drug (ribavirin, RV) as electron donor with different electron acceptors ( $I_2$ , HPA,  $H_2CA$ , DDQ), II. The nature and structure of the final products have been characterized using elemental analyses, electronic absorption spectroscopy, IR, and thermal analyses.



II. Structure of the acceptors

## EXPERIMENTAL SECTION

### Chemicals and spectral measurements

All chemicals used were of high grade. The compound 1-((2R,3R,4S,5R)-tetrahydro-3,4-dihydroxy-5-(hydroxymethyl)furan-2-yl)-1H-1,2,4-triazole-3-carboxamide (Ribavirin, RV) was obtained from Egyptian International Pharmaceutical Industry Co. (EIPICO), Egypt with purity of > 99.00% and was used without further purification. Iodine ( $I_2$ ), picric acid (HPA) chloranilic acid ( $H_2CA$ ), and 2,3-dichloro-5,6-dicyano-*p*-benzoquinone (DDQ) purchased from Merck Chemical Co. and were also used as received.

The electronic absorption spectra were recorded in region of 200-900 nm using UV-Vis. Spectrophotometer model JASCO V-530 with quartz cell of 1.00 cm path length. The infrared spectra of the reactants and the obtained complexes were recorded using KBr discs on Perkin-Elmer 1430 ratio recording Infrared spectrometer.

Elemental analyses of the dried and pure samples were carried out in microanalysis unit of Cairo University, Egypt using CHNS-932 (LECO) and Vario Elemental analysers. Chlorine was determined by burning the substance in oxygen with platinum contact and following titration with mercuric nitrate towards diphenylcarbazide. The results of elemental analyses of the solid complexes were in consistence with stoichiometric ratios obtained from photometric titrations.

Thermal analyses (TG, DTG) were carried out using a Shimadzu TGA-50 H computerized thermal analysis system. The system includes a program which processes data from the thermal analyzer with the ChromotPac C-R3A. The rate of heating of the samples was kept at 10 °C/min. Sample masses 4.475, 3.766, 3.706, 4.927 and 2.741 mg for RV and its complexes **1**, **2**, **3**, and **4**, respectively were analyzed under  $N_2$  flow at 20 ml/min.

**Spectrophotometric titration measurements**

Photometric titrations at (290, 360), (355, 395), (372, 525) and (406, 470) nm were performed for the reactions between RV and acceptors I<sub>2</sub>, HPA, H<sub>2</sub>CA, DDQ, respectively in methanol at 25°C using a Helios Gamma Unicam UV-Vis. Spectrophotometer and Jenway Visible range spectrophotometer model 6300 as follows. A 0.25, 0.50, 0.75, 1.00, 1.25, 1.5, 2.00, 2.50, 3.00 and 3.50 mL aliquot of a standard solution (1.0×10<sup>-4</sup> M) of each acceptor in MeOH was added to 1.00 mL of 1.0×10<sup>-4</sup> M RV, which was also dissolved in MeOH. The concentration of RV (C<sub>d</sub><sup>o</sup>) in the reaction mixture was maintained at 1×10<sup>-4</sup> M, while the concentrations of the acceptors (C<sub>a</sub><sup>o</sup>) were changed over a wide range of concentrations (0.25×10<sup>-4</sup> M to 3.5×10<sup>-4</sup> M) to produce solutions with an acceptor molar ratio that varied from 0.25:1.00 to 3.50:1.00. The stoichiometry of the molecular CT-complexes was obtained from the determination of the conventional spectrophotometric molar ratio according to the known method [26].

**Preparation of the solid complexes**

The solid [(RV)I]·I<sub>3</sub> (**1**), [(HRV)(PA)] (**2**), [(HRV)(HCA)] (**3**) and [(RV)(DDQ)] (**4**) complexes were prepared by adding a methanolic solution (20.0 mL) of the acceptors (2.00 mmol) to a methanolic solution (10.0 mL) of the donor RV (1.00 mmol). The resultant dark brown, scarlet-yellow, dark violet, and dark red solutions of complexes **1**, **2**, **3** and **4**, respectively were stirred for about 5 h at room temperature then left overnight to separate the solid complexes. The precipitated complexes were filtrated off, washed with MeOH (3×1/2 mL) and dried in vacuo over CaCl<sub>2</sub>.

[(RV)I]<sup>+</sup>·I<sub>3</sub><sup>-</sup> (**1**): Anal. found (Calcd. for C<sub>8</sub>H<sub>12</sub>I<sub>4</sub>N<sub>4</sub>O<sub>5</sub>, 751.82): C, 12.65 (12.78); H, 2.08 (1.61); N, 7.57 (7.45).

[(HRV)(PA)] (**2**): Anal. found (Calcd. for C<sub>14</sub>H<sub>15</sub>N<sub>7</sub>O<sub>12</sub>, 473.31): C, 35.46 (35.53); H, 3.36 (3.19); N, 20.55 (20.72).

[(HRV)(HCA)] (**3**): Anal. found (Calcd. for C<sub>14</sub>H<sub>14</sub>Cl<sub>2</sub>N<sub>4</sub>O<sub>9</sub>, 453.19): C, 37.05 (37.10); H, 3.46, (3.11); Cl, 16.00 (15.65); N, 12.48 (12.36).

[(RV)(DDQ)] (**4**): Anal. found (Calcd. for C<sub>16</sub>H<sub>12</sub>Cl<sub>2</sub>N<sub>6</sub>O<sub>7</sub>, 471.21): C, 40.75 (40.78); H, 2.90 (2.57); Cl, 15.77 (15.05); N, 17.91 (17.84).

**Antibacterial activity**

The antimicrobial activities of the CT complexes with rebavirin and the pure solvent were tested *in vitro* against bacterial strains (*Pseudomonas aeruginosa*, *Staphylococcus aureus*, *Bacillus subtilis*, *Escherichia coli*) using agar well diffusion method. The samples were dissolved in DMSO to make a concentration of 100 µg/mL. The inoculum (1×10<sup>8</sup> Cfu/mL) was added to molten agar and the media were shaken to disperse the microorganisms. Four millimeters diameter wells were punched in the agar with a sterile cork borer. A 10 µL of the sample was introduced in the well. Antimicrobial activity was evaluated by measuring the diameter of inhibition zone in mm [27,28].

**RESULTS AND DISCUSSION****Electronic spectra**

Electronic absorption spectra of the donor RV and of the formed CT-complexes are shown in Fig. 1. These spectra have revealed new strong absorption bands attributed to the CT-interactions. These bands are not present in the spectra of the free reactants and are observed at (290, 360), (355, 395), (372, 525), (406, 470) nm for the complexes, [(RV)I]·I<sub>3</sub> (**1**), [(HRV)(PA)] (**2**), [(HRV)(HCA)] (**3**) and [(RV)(DDQ)] (**4**), respectively. Polyiodides (I<sub>n</sub> when n=3, 5, 7) are characterized by the appearance of two absorption bands in the electronic spectrum of the iodine complex **1** [29-32]. The data obtained indicate the presence of I<sub>3</sub><sup>-</sup> species in the polyiodide unit. The formation of triiodide with RV in which I<sup>+</sup> is included in the organic moiety of RV is shown in the following proposed mechanism:

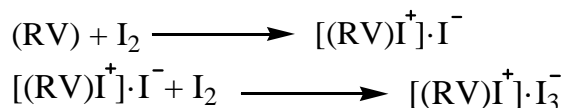
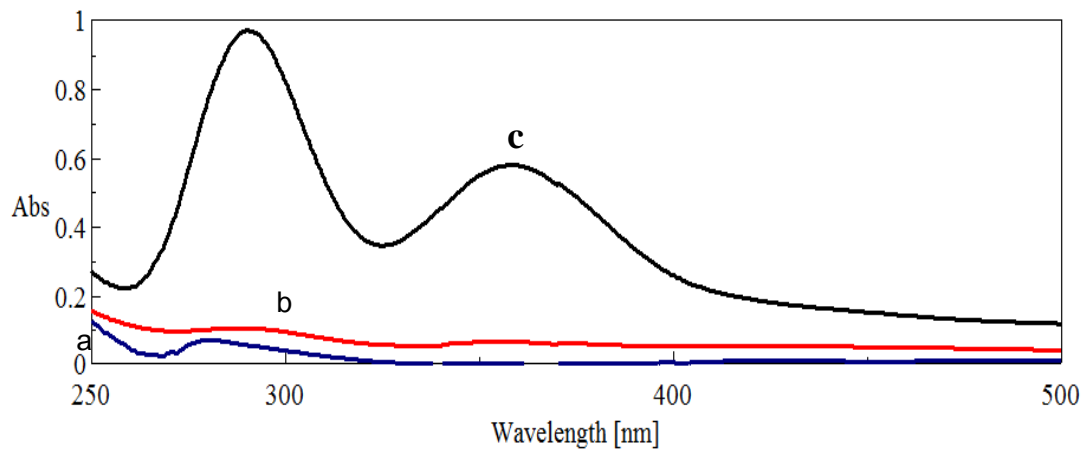
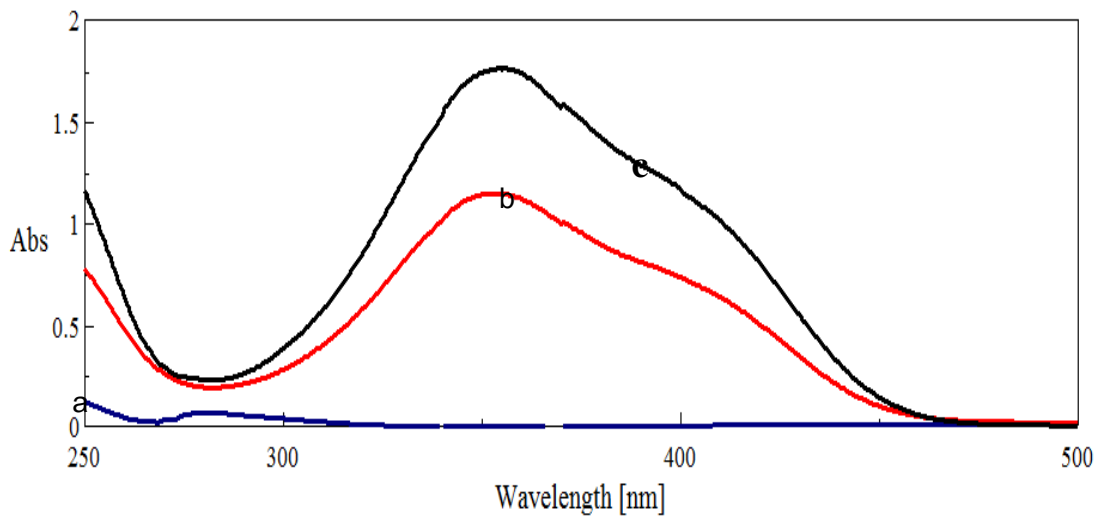


Fig. 1. Electronic absorption spectra of:

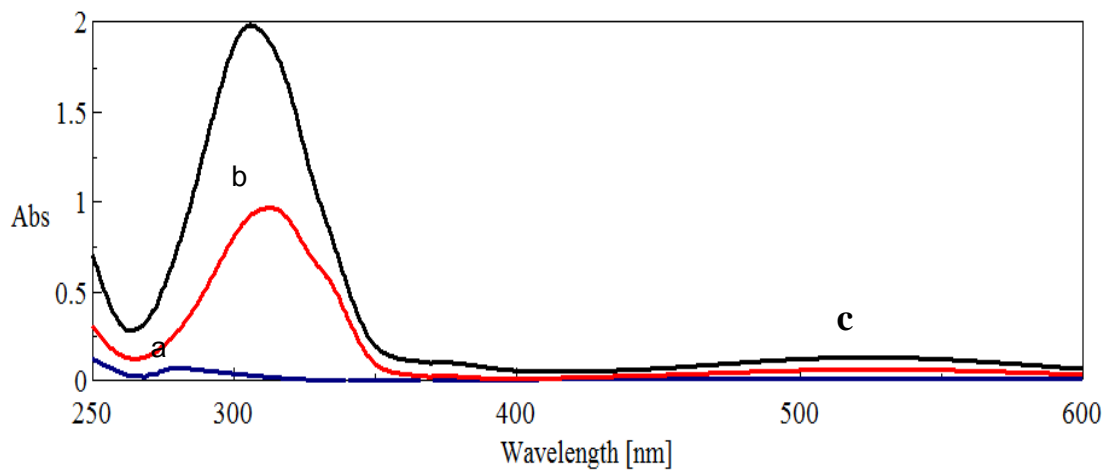
(A): RV-I<sub>2</sub> reaction in MeOH

(a: [RV] = 1.0 × 10<sup>-4</sup> M, b: [I<sub>2</sub>] = 1.0 × 10<sup>-4</sup> M and c: [RV-I<sub>2</sub> product] = 1.0 × 10<sup>-4</sup> M).

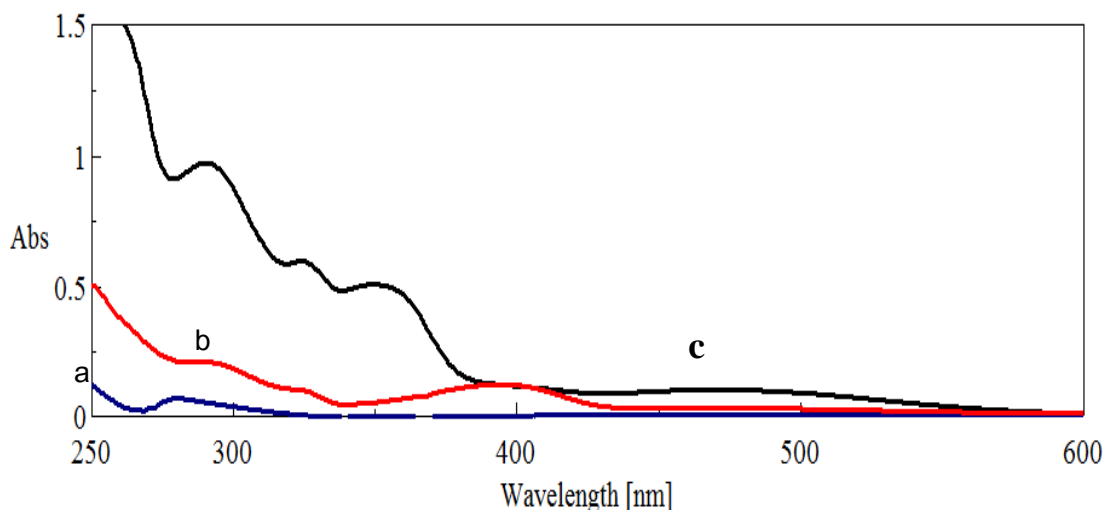


(B): RV-HPA reaction in MeOH

(a: [RV] = 1.0 × 10<sup>-4</sup> M, b: [HPA] = 1.0 × 10<sup>-4</sup> M and c: [RV-HPA product] = 1.0 × 10<sup>-4</sup> M).

(C): RV-H<sub>2</sub>CA reaction

(a: [RV] = 1.0 × 10<sup>-4</sup> M, b: [H<sub>2</sub>CA] = 1.0 × 10<sup>-4</sup> M and c: [RV-H<sub>2</sub>CA product] = 1.0 × 10<sup>-4</sup> M).



(D): RV-DDQ reaction

(a:  $[RV] = 1.0 \times 10^{-4} M$ , b:  $[DDQ] = 1.0 \times 10^{-4} M$  and c:  $[RV-DDQ \text{ product}] = 1.0 \times 10^{-4} M$ ).

Photometric titration measurements based on these characteristic CT-absorption bands of the CT-complexes, Fig. 2, confirmed the complex formation in a ratio, RV: acceptor of 1:2 for complex **1** and 1:1 for complexes **2–4** [33]. The obtained spectrophotometric data, Tables 1 and 2(A-C) were used to calculate the values of both equilibrium constants,  $K_{CT}$ , and extinction coefficient,  $\epsilon$  of the CT-complexes in MeOH for  $[(RV)I] \cdot I_3$ ,  $[(HRV)(PA)]$ ,  $[(HRV)(HCA)]$  and  $[(RV)(DDQ)]$  complexes based on the known equation (1) for the 1:2 stoichiometry [34] and equation (2) for the 1:1 stoichiometry [35].

$$\frac{C_d^\circ \cdot C_a^{\circ 2}}{A} = \frac{1}{\epsilon K_c} + \frac{C_a^\circ (4C_d^\circ + C_a^\circ)}{\epsilon} \quad (1)$$

$$\frac{C_d^\circ \cdot C_a^\circ}{A} = \frac{1}{\epsilon K_c} + \frac{C_d^\circ + C_a^\circ}{\epsilon} \quad (2)$$

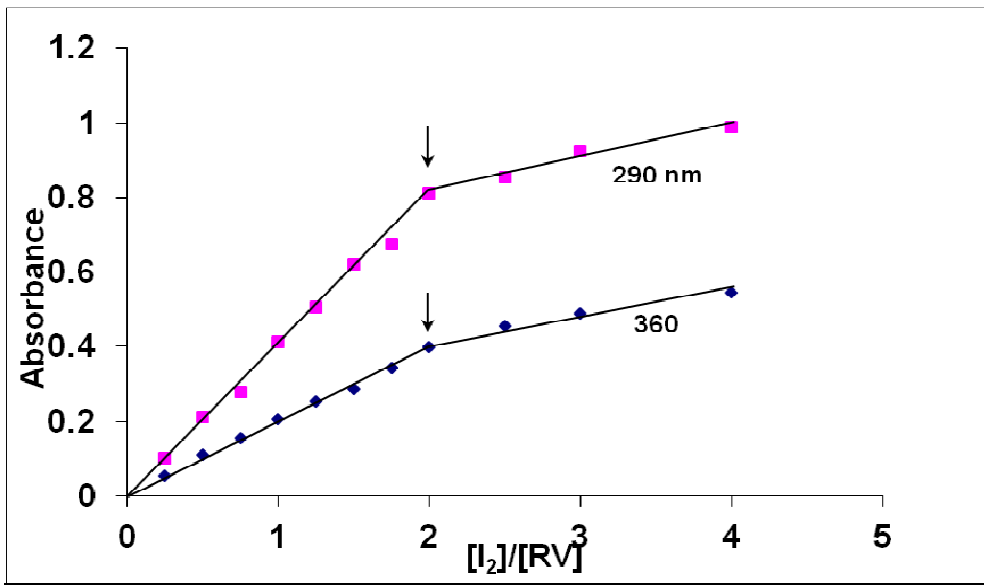
where  $C_a^\circ$  and  $C_d^\circ$  are initial concentration of the acceptors ( $I_2$ , HPA,  $H_2CA$ , DDQ) and donor RV, respectively.

A is the absorbance of new strong bands at (290, 360), (355, 395), (372, 525), (406, 470) nm.

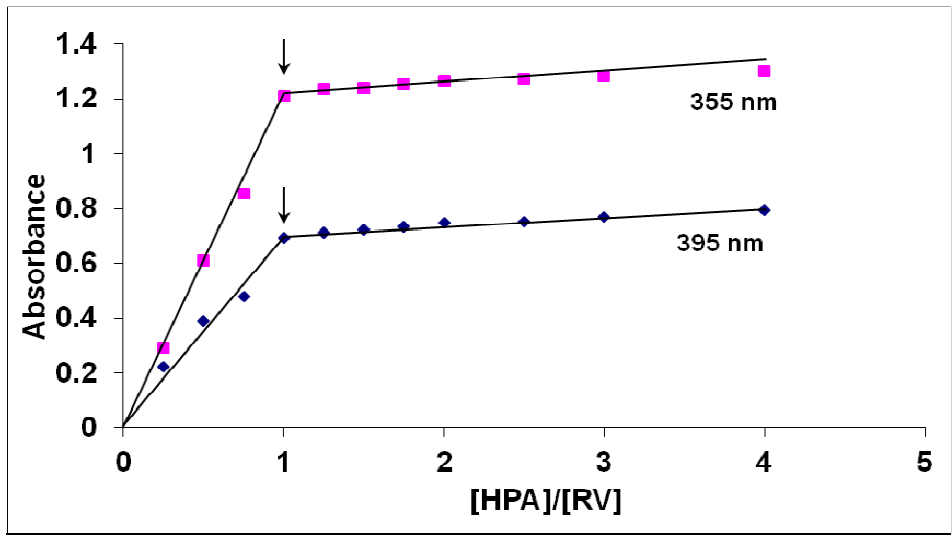
When  $(C_d^\circ \cdot C_a^{\circ 2} / A)$  are plotted against  $C_a^\circ (4C_d^\circ + C_a^\circ)$  for complex **1** and  $C_d^\circ \cdot C_a^\circ / A$  are plotted against  $(C_d^\circ + C_a^\circ)$  for complexes **2–4**, straight lines are obtained with a slope of  $1/\epsilon$  and intercept of  $1/\epsilon K_c$ .

Some spectroscopic and physical parameters such as standard free energy ( $\Delta G^\circ$ ), transition dipole moment ( $\mu$ ), oscillator strength ( $f$ ) and the ionization potential ( $I_D$ ) were estimated for complexes dissolved in MeOH at 25°C and summarized in Table 3.

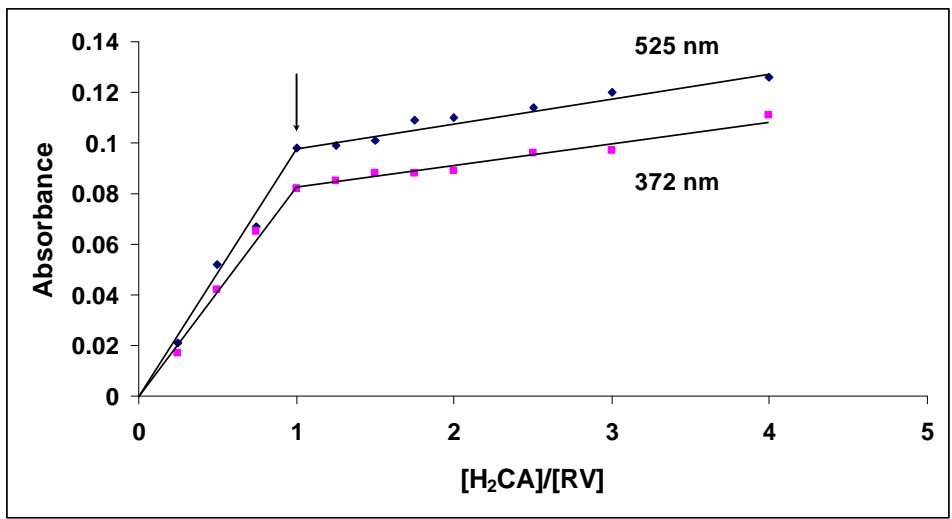
Fig. 2. Photometric titration curves for RV–Acceptor reactions in MeOH at room temperature:



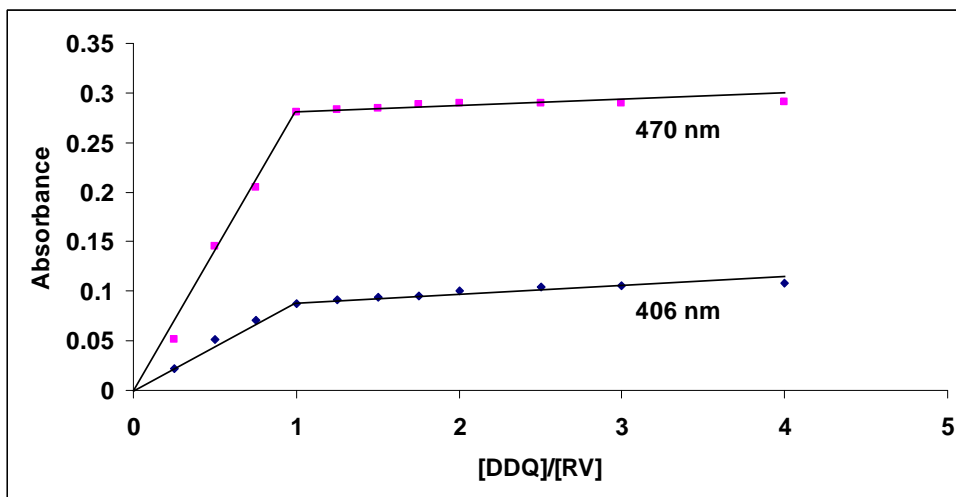
(A): RV–I<sub>2</sub> reaction; 290, 360 nm bands



(B): RV–HPA reaction; 355, 395 nm bands



(C): RV–H<sub>2</sub>CA reaction; 372, 525 nm bands



(D): RV-DDQ reaction; 406, 470 nm bands

Table 1. Molar concentrations for (RV) with the acceptors in the reaction mixtures

Base conc., $\times 10^{-4}$ M	Acceptor	Concentration range of the acceptors, M	Acceptor-base molar ratio
1.00	I <sub>2</sub>	$0.25 \times 10^{-4} - 4 \times 10^{-4}$	0.25: 1.00 - 4.00:1.00
1.00	HPA	$0.25 \times 10^{-4} - 4 \times 10^{-4}$	0.25: 1.00 - 4.00:1.00
1.00	H <sub>2</sub> CA	$0.25 \times 10^{-4} - 4 \times 10^{-4}$	0.25: 1.00 - 4.00:1.00
1.00	DDQ	$0.25 \times 10^{-4} - 4 \times 10^{-4}$	0.25: 1.00 - 4.00:1.00

Table 2A. The Values of  $C_d^\circ \cdot C_a^{\circ 2} / A$  and  $C_a^\circ (4C_d^\circ + C_a^\circ)$  for complex 1

$V_a$ , ml ( $5.00 \times 10^{-4}$ M)*	$C_a^\circ$ , $\times 10^{-4}$	Ratio (a/d)	A		$C_a^\circ (4C_d^\circ + C_a^\circ)$ , $\times 10^{-8}$	$C_d^\circ \cdot C_a^{\circ 2} / A$ , $\times 10^{-12}$	
			1,	1,		1,	1,
			290 nm	360 nm		290 nm	360 nm
0.25	0.25	0.25	0.101	0.055	1.063	6.188	1.136
0.50	0.50	0.50	0.211	0.11	2.250	11.848	2.273
0.75	0.75	0.75	0.278	0.156	3.563	2.023	3.606
1.00	1.00	1.00	0.415	0.205	5.000	2.409	4.878
1.25	1.25	1.25	0.505	0.255	6.563	3.109	6.127
1.50	1.50	1.50	0.620	0.288	8.250	3.629	7.813
1.75	1.75	1.75	0.675	0.345	10.063	4.537	8.877
2.00	2.00	2.00	0.811	0.399	12.000	4.932	10.025
2.50	2.50	2.50	0.855	0.456	16.250	7.309	13.706
3.00	3.00	3.00	0.925	0.489	21.000	9.729	18.405
4.00	4.00	4.00	0.989	0.545	32.000	16.178	29.358

\* $V_a$  is 1 ml ( $5.00 \times 10^{-4}$  M);  $C_d^\circ$  is  $1.00 \times 10^{-4}$  M in all systems.

Table 2B. The Values of  $C_d^\circ \cdot C_a^\circ / A$  and  $C_d^\circ + C_a^\circ$  for complexes 2 and 3

$V_a$ , ml ( $5.00 \times 10^{-4}$ M)*	$C_a^\circ$ , $\times 10^{-4}$	Ratio (a/d)	A				$C_d^\circ + C_a^\circ$ , $\times 10^{-4}$	$C_d^\circ \cdot C_a^\circ$ , $\times 10^{-8}$	$C_d^\circ \cdot C_a^\circ / A$ , $\times 10^{-8}$			
			2,	2,	3,	3,			2,	2,	3,	3,
			395 nm	355 nm	525 nm	372 nm			355 nm	395 nm	525 nm	372 nm
0.25	0.25	0.25	0.223	0.292	0.021	0.017	1.25	0.25	0.856	1.121	11.905	14.706
0.50	0.50	0.50	0.39	0.611	0.052	0.042	1.50	0.50	0.818	1.282	9.615	11.905
0.75	0.75	0.75	0.481	0.851	0.067	0.065	1.75	0.75	0.881	1.559	11.194	11.538
1.00	1.00	1.00	0.692	1.211	0.098	0.082	2.00	1.00	0.826	1.445	10.204	12.195
1.25	1.25	1.25	0.711	1.235	0.099	0.085	2.25	1.25	1.012	1.758	12.626	14.706
1.50	1.50	1.50	0.723	1.241	0.101	0.088	2.50	1.50	1.209	2.075	14.851	17.045
1.75	1.75	1.75	0.734	1.255	0.109	0.088	2.75	1.75	1.394	2.384	16.055	19.886
2.00	2.00	2.00	0.746	1.266	0.110	0.089	3.00	2.00	1.579	2.681	18.181	22.472
2.50	2.50	2.50	0.752	1.273	0.114	0.096	3.50	2.50	1.964	3.324	21.929	26.042
3.00	3.00	3.00	0.771	1.284	0.120	0.097	4.00	3.00	2.336	3.891	25.000	30.928
4.00	4.00	4.00	0.794	1.301	0.126	0.111	5.00	4.00	3.075	5.037	31.746	36.036

\* $V_a$  is 1 ml ( $5.00 \times 10^{-4}$  M);  $C_d^\circ$  is  $1.00 \times 10^{-4}$  M in all systems.

Table 2C. The Values of  $C_d^\circ \cdot C_a^\circ / A$  and  $C_d^\circ + C_a^\circ$  for complex 4

$V_a, \text{ml}$ ( $5.00 \times 10^{-4} \text{M}$ ) <sup>*</sup>	$C_a^\circ$ , $\times 10^{-4}$	Ratio ( $a/d$ )	A		$C_d^\circ + C_a^\circ$ , $\times 10^{-4}$	$C_d^\circ \cdot C_a^\circ$ , $\times 10^{-8}$	$C_d^\circ \cdot C_a^\circ / A$ , $\times 10^{-8}$	
			4,	4,			4,	4,
			406 nm	470 nm			406 nm	470 nm
0.25	0.25	0.25	0.022	0.051	1.25	0.25	11.364	4.902
0.50	0.50	0.50	0.051	0.145	1.50	0.50	9.804	3.448
0.75	0.75	0.75	0.071	0.205	1.75	0.75	10.563	3.659
1.00	1.00	1.00	0.088	0.281	2.00	1.00	11.364	3.559
1.25	1.25	1.25	0.091	0.283	2.25	1.25	13.736	4.417
1.50	1.50	1.50	0.094	0.285	2.50	1.50	15.957	5.263
1.75	1.75	1.75	0.095	0.288	2.75	1.75	18.421	6.076
2.00	2.00	2.00	0.101	0.289	3.00	2.00	19.802	6.920
2.50	2.50	2.50	0.104	0.289	3.50	2.50	24.038	8.651
3.00	3.00	3.00	0.105	0.290	4.00	3.00	28.571	10.345
4.00	4.00	4.00	0.108	0.291	5.00	4.00	37.037	13.746

<sup>\*</sup> $V_a$  is 1 ml ( $5.00 \times 10^{-4} \text{M}$ );  $C_d^\circ$  is  $1.00 \times 10^{-4} \text{M}$  in all systems.

Fig. 3A. Relation between  $C_d^\circ \cdot C_a^{\circ 2} / A$  and  $C_a^\circ (4C_d^\circ + C_a^\circ)$  for RV-I<sub>2</sub> system in MeOH at 290 and 365 nm

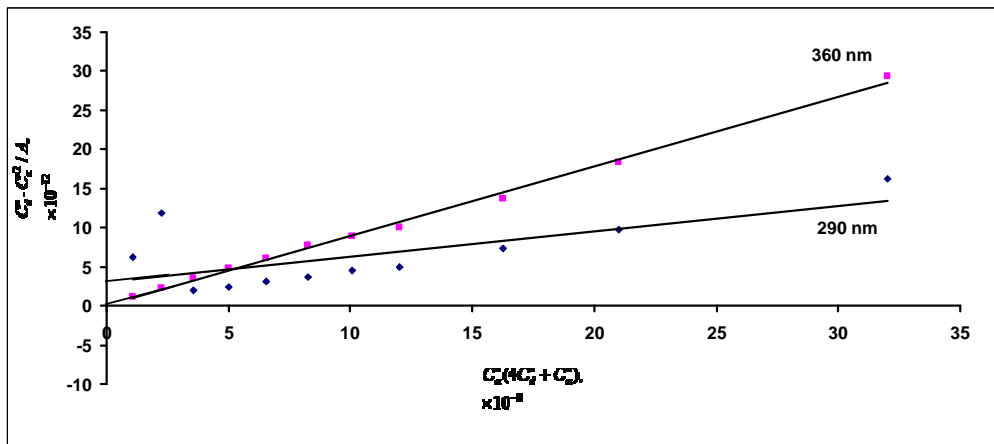
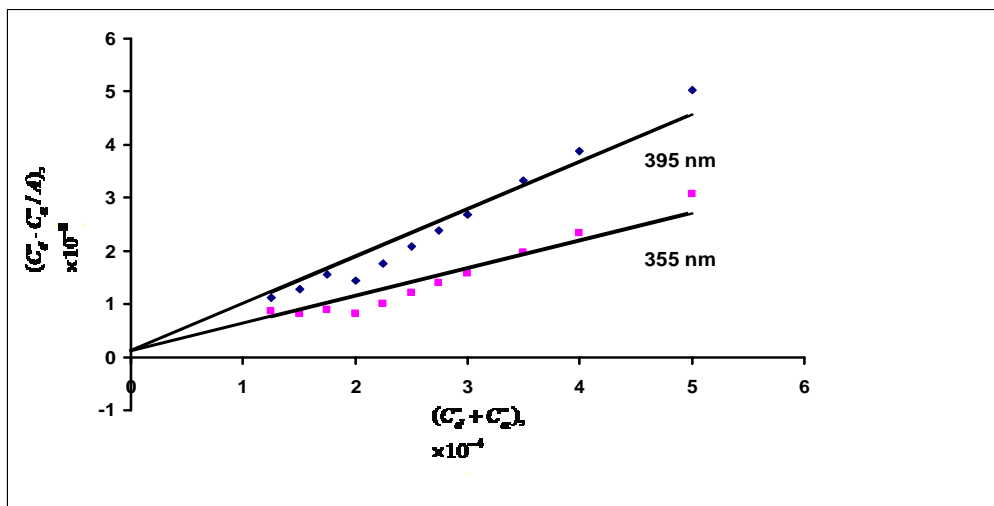
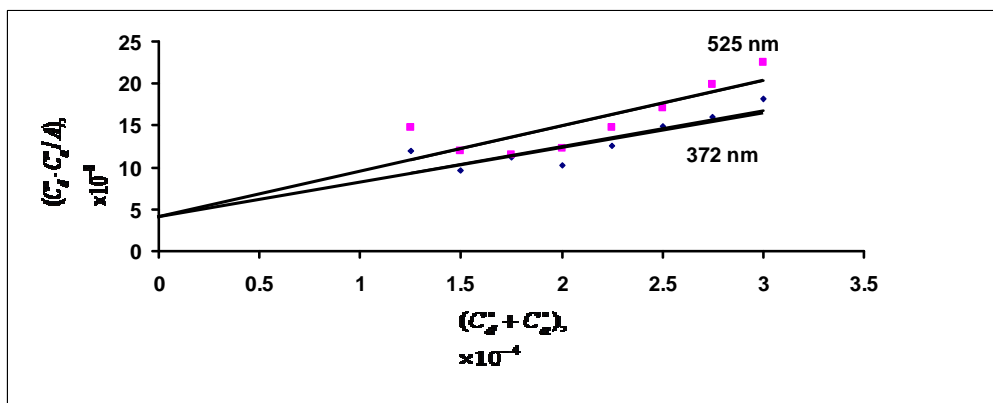
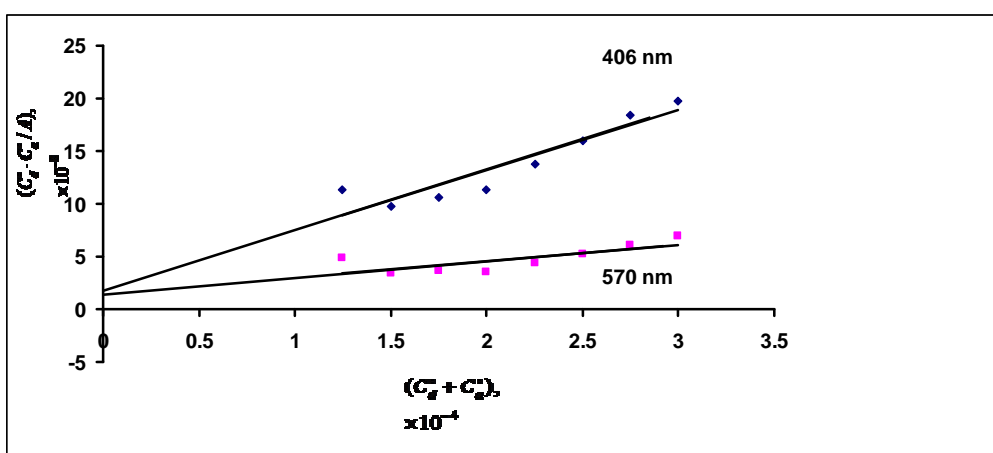


Fig. 3B. Relation between  $C_d^\circ \cdot C_a^\circ / A$  and  $C_d^\circ + C_a^\circ$  for:



(B) RV-HPA system in MeOH at 355 and 395 nm

(C) RV-H<sub>2</sub>CA system in MeOH at 372 and 525 nm

(D) RV-DDQ system in MeOH at 406 and 570 nm

The oscillator strength ( $f$ ) is a dimensionless quantity used to express the transition probability of the CT band. From the CT absorption spectra, the oscillator strength ( $f$ ) can be estimated by equation 3 [36].

$$f = 4.319 \times 10^{-9} (\epsilon_{\max} \cdot \Delta \nu_{1/2}) \quad (3)$$

where  $\epsilon_{\max}$  is the maximum extinction coefficient of the CT band, and  $\Delta \nu_{1/2}$  is the half-bandwidth in  $\text{cm}^{-1}$  (i.e., the bandwidth at half of the maximum extinction coefficient value).

The transition dipole moments ( $\mu$ ) of the RV CT-complexes have been calculated from equation 4 [37].

$$\mu_{(Debye)} = 0.958 \left( \frac{\epsilon_{\max} \cdot \Delta \nu_{1/2}}{\nu_{\max}} \right)^{1/2} \quad (4)$$

The transition dipole moment can be used to determine if a particular transition is allowed; the transition from a bonding  $\pi$ -orbital to an antibonding  $\pi^*$  orbital is allowed because the integral that defines the transition dipole moment is nonzero.

The ionization potentials ( $I_D$ ) of the RV donor in the CT complexes were calculated using the empirical equation (5) derived by Aloisi and Pignataro [38].

$$I_{D(eV)} = 5.76 + 1.53 \times 10^{-4} \cdot \nu_{CT} \quad (5)$$

where  $\nu_{CT}$  is the wavenumber in  $\text{cm}^{-1}$  that corresponds to the CT band formed from the interaction between the donor and the acceptor. The electron-donating power of a donor molecule is measured by its ionization potential, which is the energy required to remove electron from the highest occupied molecular orbital.

The energy values ( $E_{CT}$ ) of the  $n$  to  $\pi^*$  and  $\pi$ - $\pi^*$  interactions between the donor (RV) and the acceptors were calculated using equation 6 derived by Briegleb [39].

$$E_{CT} = (h\nu_{CT}) = 1243.667 / \lambda_{CT(\text{nm})} \quad (6)$$

where  $\lambda_{CT}$  is a wavelength of the CT band.

The standard free energy of complexation  $\Delta G^\circ$  for each complex was calculated using equation 7 [40].

$$\Delta G^\circ = -2.303RT \log K_{CT} \quad (7)$$

The obtained data in Table 3 showed that, the complexes [(RV)I] $\cdot$ I<sub>3</sub> and [(HRV)(PA)] exhibit considerably higher values of both the oscillator strength ( $f$ ) and the transition dipole moment ( $\mu$ ) which indicated a strong interaction between the donor-acceptor pairs with relatively high probabilities of CT transitions [41]. Also, in complex **1** a relatively higher degree of ionization potential of the donor is observed. The obtained negative values of  $\Delta G^\circ$  for the CT-complexes indicate that the interaction between the drug and acceptors is exothermic and spontaneous [42,43].

Table 3. Spectrophotometric results for RV CT-complexes in MeOH

Complex	$\lambda_{\text{max}}$ (nm)	$K_C$ ( $\text{l}\cdot\text{mol}^{-1}$ )	$\epsilon_{\text{max}}$ ( $\text{l}\cdot\text{mol}^{-1}\cdot\text{cm}^{-1}$ )	$E_{CT}$ (eV)	$f$	$\mu$	$I_p$ (ev)	$\Delta G^\circ$ (25°C) ( $\text{K}\cdot\text{J}\cdot\text{mol}^{-1}$ )
[(RV)I] $\cdot$ I <sub>3</sub>	290	$0.10 \times 10^4$	$0.32 \times 10^4$	4.29	4.15 11.23	16.10	10.96	$-1.72 \times 10^4$
	360	$7.22 \times 10^4$	$1.13 \times 10^4$	3.46		29.19	10.04	$-2.77 \times 10^4$
[(HRV)(PA)]	355	$5.22 \times 10^4$	$1.92 \times 10^4$	3.50	16.58	37.55	9.59	$-2.69 \times 10^4$
	395	$8.93 \times 10^4$	$1.12 \times 10^4$	3.15	13.54	37.94	9.59	$-2.82 \times 10^4$
[(HRV)(HCA)]	372	$1.06 \times 10^4$	$0.23 \times 10^4$	3.34	2.29	13.41	9.89	$-2.30 \times 10^4$
	525	$1.32 \times 10^4$	$0.19 \times 10^4$	2.37	0.93	10.21	8.67	$-2.35 \times 10^4$
[(RV)(DDQ)]	406	$3.46 \times 10^4$	$0.17 \times 10^4$	3.06	1.54	11.45	9.59	$-2.59 \times 10^4$
	470	$1.08 \times 10^4$	$0.64 \times 10^4$	2.65	4.69	21.81	8.97	$-2.30 \times 10^4$

### IR Spectra

IR spectra of reactants and the obtained products are given in Fig. 4 and the assignments of their characteristic bands are given in Table 4. The formation of CT-complexes during the reaction of RV with I<sub>2</sub>, picric acid, chloranilic acid and DDQ is strongly supported by observing of main infrared bands of the donor (RV) and acceptors (HPA, H<sub>2</sub>CA, DDQ) in the product spectra. However, the bands of the donor and acceptors in the complexes spectra reveal small shifts in wavenumber values and intensities compared with those of the free donor and acceptors. This should be attributed to the expected symmetry and electronic structure changes upon the formation of CT-complexes.

For acid-base interaction, a proton transfer from the acceptor (acid) to the donor (base) is expected to occur. This seems to be liable to occur in the case of RV interaction with picric and chloranilic acids. Such assumption is strongly supported as follow; the spectrum of free donor reveals to absorption peaks at 3448 and 3349  $\text{cm}^{-1}$  which is characteristic to the presence of an -NH<sub>2</sub> and -OH groups are slightly shifted toward lower frequencies. This small shift was attributed to the presence of many hydroxo groups, hydrogen bond formation and the (N-H) stretching vibration of hydrogen against positively charged nitrogen. We may suggest that, the acid-base interaction is associated with a proton migration followed by hydrogen bonding formation. The RV-HPA and RV-H<sub>2</sub>CA interaction involves a protonation for the basic nitrogen of the CFX nitrogens. Accordingly, we may formulate the complex as [(HRV)<sup>+</sup>(PA)]<sup>-</sup>, [(HRV)<sup>+</sup>(HCA)]<sup>-</sup>. Due to the increased electron density on the picrate and chloranilate units as a result of charge transfer interaction and deprotonation of the acids upon complexation, the shift of  $\nu_{as}(\text{NO}_2)$  of the picric acid and  $\nu(\text{C}-\text{Cl})$  of chloranilic acid to lower frequencies upon complexation can be attributed [44-47].

The IR spectrum of free DDQ shows CN stretching frequencies at 2243  $\text{cm}^{-1}$ . The significant shift of this vibration toward lower frequency (2225  $\text{cm}^{-1}$ ) on complexation is indicative of charge transfer from RV to  $\pi$  of a C $\equiv$ N group of DDQ which leads to a weakening of this bond. The C=O systems of the free donor did not show a remarkable change upon complexation which mean that it did not participate in complex formation while the C=O systems of

the quinones in acceptor goes to lower frequencies upon complexation with DDQ and this is in consistence with the increased electron density on the acceptor upon complexation [46-50].

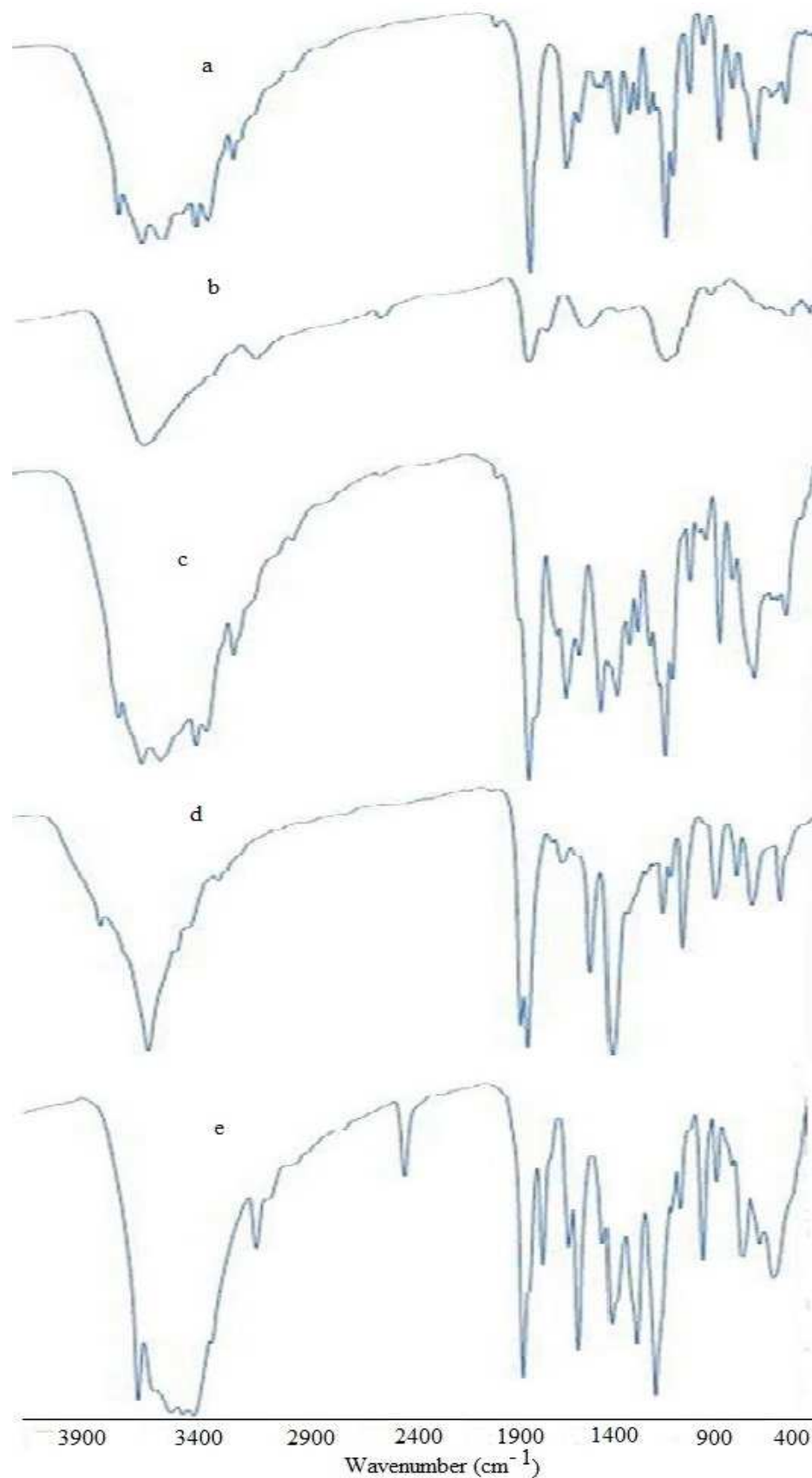


Fig. 4. Infrared spectra of (a) RV donor and its CT-complexes (b) complex 1, (c) complex 2, (d) complex 3 and (e) complex 4

Table 4. Characteristic infrared frequencies\* (cm<sup>-1</sup>) and tentative assignments for RV and its CT-complexes

RV	HPA	H <sub>2</sub> CA	DDQ	Complex 1	Complex 2	Complex 3	Complex 4	Assignments
3448 s 3349 s,br	3433 br	3235 w	3442 w 3339 w	3420 vs,br	3445 s 3345 vs	3446 m 3345 sh	3474 vs 3405 sh 3322 s	v(N-H), v(O-H), H bonded v(N <sup>+</sup> -H); of NH <sub>2</sub>
3262 s 3179 m 3117 s 3066 s					3270 sh 3110 sh	3265 vs 3113 s 3069 s	3238 vs,br 3268 s 3224 s 3145 sh	v(C-H), aromatic
2950 m 2920 sh	2976 sh 2873 w			2924 m	2950 m 2918 sh	2953 m	2935 m	v <sub>s</sub> (C-H) + v <sub>as</sub> (C-H)
1793 w			2243 m		1793 sh	1793 vw	2225 m 1704 vs	v(C≡N), DDQ v(C=O), amide
1658 vs		1665 s	1673 vs	1691 s 1609 m	1657 vs 1628 sh 1558 vs	1661 s 1630 vs	1678 sh 1614 s	v(C=O), amide, quinone
1495 s 1437 m	1607 vs 1347 ms	1368 vs	1358 s	1436 m	1532 m	1533 vw	1495 m	v <sub>as</sub> (NO <sub>2</sub> ) v(C=C) stretch, v(C=N) stretch
1356 m 1334 w					1495 s 1436 m 1342 s 1277 s	1494 w 1367 m	1451 s 1341 w	v(C-H) Plane bending
1278 m 1221 m 1187 m 1134 w 1067 vs 1034 m 957 m 895 w 828 m	1316 ms 1147 ms	1369 m 1290 vs	1268 ms 1216 w	1293 w 1087 s 877 w	1133 w 1067 vs 1035 m 957 w 913 w 886 w 827 m	1271 s 1213 w 1036 w 981 m	1299 s 1187 s 1100 vs 1027 vw 987w 882 m 818 w	v(C-N) v(C-O)
	1083 ms							v <sub>s</sub> (NO <sub>2</sub> ), HPA v(C-Cl)
760 w 673 m		856 m 690 m	796 s	628 w	771 w 675 m	755 w 687 m	748 w 696 m 620 w	CH <sub>2</sub> rocking
538 w	783 s 733 s 698 s 646 sh 550 m	571 ms	615 s	521 w	622 w	567 m	557 m	(C-H) out of plane
					538 m 470 w			δ(ONO): HPA

\*: s, strong; w, weak; m, medium; sh, shoulder; v, very; br, broad.

### Thermal analysis

The proposed structures for the complexes under investigation were confirmed by measuring TGA, and DTG thermograms (Fig. 5) under nitrogen flow. The thermal data obtained for complexes **1**, **2**, **3** and **4** together with the free donor, RV are summarized and given in Table 5.

The free RV decomposes in two steps at 272°C and 670°C. The total weight loss associated with these steps of decomposition is close to the theoretical calculation. The decomposition mode of the complexes under investigation occurs in a similar manner.

The decomposition reactions of complex **1** occur in two closed main stages. The first stage of decomposition occurs in one step at 156°C with a weight loss of 69.00% and the second stage at 227°C with a weight loss of 31.00%. These values of weight loss may be due to the loss of two iodine molecules and organic moiety of the donor (RV) in good agreement with the calculated values of 67.52% and 32.48%, respectively.

In complex **2**, the decomposition reactions occur in two main stages. The first stage of decomposition occurs in two steps at 189 and 253°C with a weight loss of 53.02%. This value of weight loss may be due to the loss of (HRV<sup>+</sup>) organic moiety in agreement with the calculated value of 51.81%. The second stage of decomposition occurs in one step at 710°C with a weight loss of 46.98%. This value of weight loss may be due to the loss of (PA<sup>-</sup>) organic moiety in agreement with the calculated value of 48.19%. In complex **3**, the decomposition reactions occur at two closed stages, observed at 186°C and 241°C which may be attributed to the loss of the donor and the acceptor organic moieties of the complex. The found and calculated weight loss values are in good agreements.

In complex **4**, the decomposition reactions occur in two main stages and each at 224 and 644°C with a weight loss of 52.45% and 47.55%. These values of weight loss may be due to the loss of (RV) and (DDQ) organic moieties in good agreement with the calculated values of 51.83% and 48.17%, respectively [51].

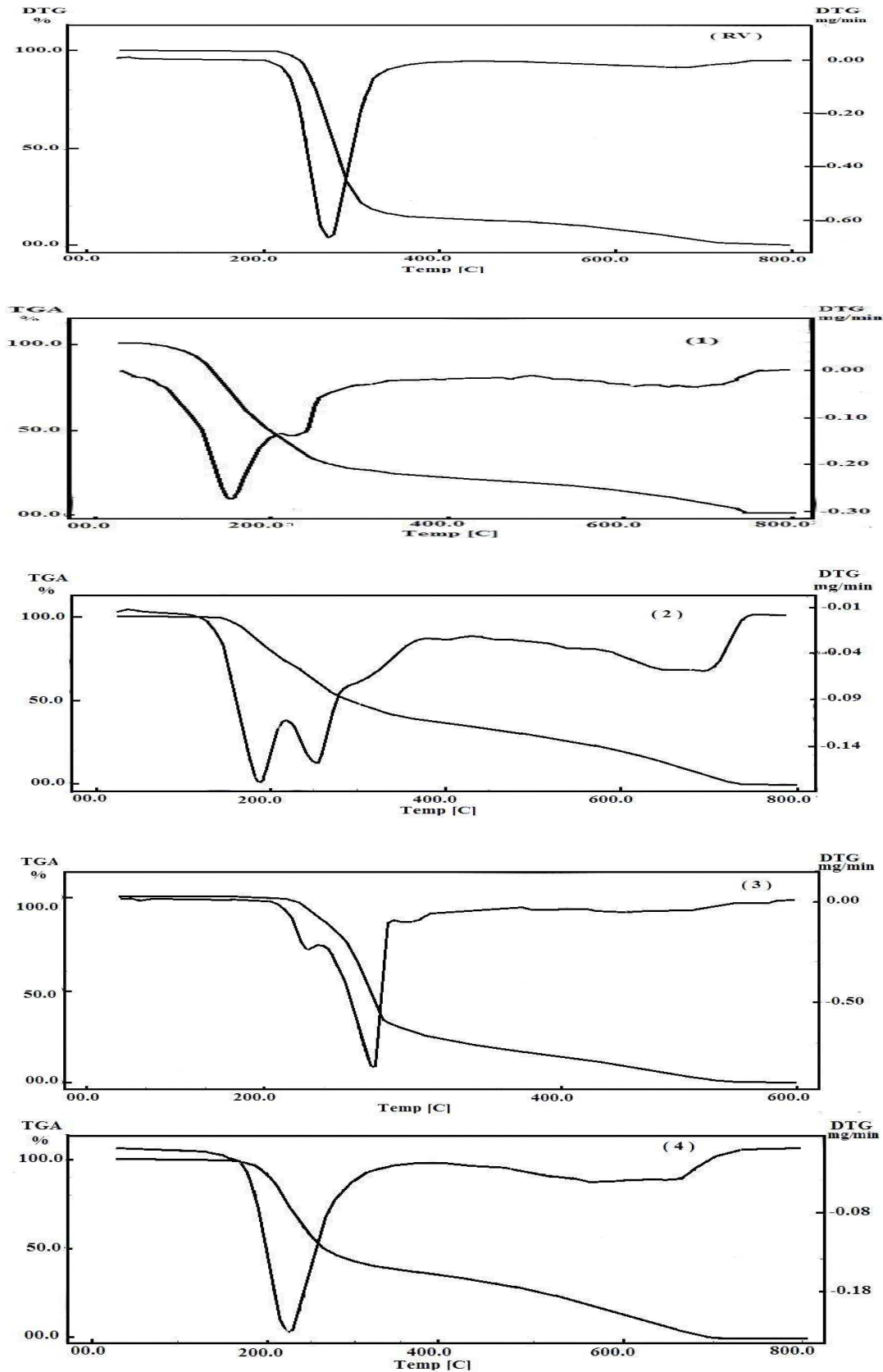


Fig. 5. Thermogravimetric (TGA) and derivative (DTG) of RV and its complexes

**Table 5. The maximum temperature values for the decomposition along with the species lost in each step of the decomposition reaction of the free RV and its CT-complexes**

Compound	Decomposition	$T_{max}/^{\circ}C$	Lost species	% Weight loss	
				Found	Calc.
RV	First stage	272	$C_8H_{12}N_4O_5$	87.10	100.00
	Second stage	670		12.90	
	Total loss			100.00	100.00
	Residue			00.00	00.00
[(RV)I] <sup>+</sup> ·I <sub>3</sub> <sup>-</sup> (1)	First main stage	156	$C_8H_{12}N_4O_5$	69.00	67.52
	Second stage	227		31.00	32.48
	Total loss			100.00	100.00
	Residue			00.00	00.00
[(HRV)(PA)] (2)	First stage	189 253	$C_8H_{13}N_4O_5$	53.02	51.81
	Second stage	710		46.98	48.19
	Total loss			100.00	100.00
	Residue			00.00	00.00
[(HRV)(HCA)] (3)	First step	186	$C_8H_{13}N_4O_5$	55.97	54.11
	Second step	241		44.03	45.89
	Total loss			100.00	100.00
	Residue			00.00	00.00
[(RV)(DDQ)] (4)	First stage	224	$C_8H_{12}N_4O_5$	52.45	51.83
	Second stage	644		47.55	48.17
	Total loss			100.00	100.00
	Residue			00.00	00.00

### Antibacterial activity

The antibacterial activity of the CT-complexes with rebavirin were screened *in vitro* against two gram-positive bacterial strains, *Staphylococcus aureus* and *Bacillus subtilis*, and two gram-negative bacterial strains, *Escherichia coli* and *Pseudomonas aeruginosa*. The activity was determined by measuring the inhibition zone diameter values (mm) of the complexes against the microorganisms. Ampicillin was used as the positive control. The screening data are listed in Table 6. The results indicated that the rebavirin CT-complexes exhibited moderate inhibitory results against all of the gram-positive and gram-negative bacterial species. It is obvious that the antibacterial activities of the CT-complexes are lower than Ampicillin standard and complex 2 have the higher antibacterial activity than other complexes.

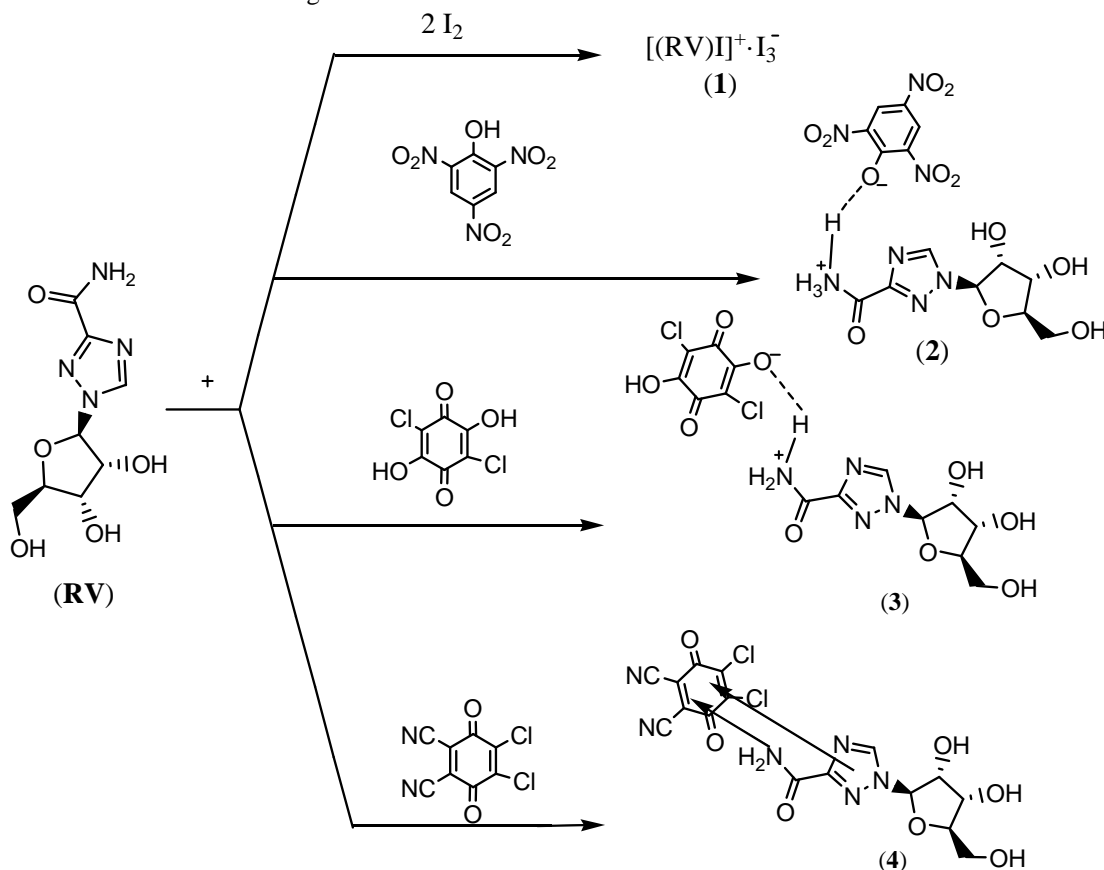
**Table 6. Antibacterial activity (inhibition zone diameter in mm) of RV CT-complexes**

Sample	Bacteria			
	<i>Bacillus subtilis</i> , G <sup>+</sup>	<i>Staphylococcus aureus</i> , G <sup>+</sup>	<i>Escherichia coli</i> , G <sup>-</sup>	<i>Pseudomonas aeruginosa</i> , G <sup>-</sup>
DMSO	0.0	0.0	0.0	0.0
Ampicilin	22	23	23	21
Complex 1	18	19	18	17
Complex 2	19	20	19	18
Complex 3	14	15	14	15
Complex 4	17	17	15	15

### CONCLUSION

Charge transfer interactions between the donor (RV) with the  $\sigma$ -acceptor like I<sub>2</sub> and  $\pi$ -acceptors such as HPA, H<sub>2</sub>CA and DDQ were studied in MeOH at 25°C. The synthesized CT-complexes were characterized using various spectroscopic techniques including UV-visible, and IR spectroscopy and confirmed by elemental and thermal analyses. The reactions stoichiometries were found to be 1:2 for complex 1 and 1:1 for complexes 2–4 and had the formulas: [(RV)I]<sup>+</sup>·I<sub>3</sub><sup>-</sup> (1), [(HRV)<sup>+</sup>(PA)]<sup>-</sup> (2), [(HRV)<sup>+</sup>(HCA)]<sup>-</sup> (3) and [(RV)(DDQ)] (4). Reaction of RV with iodine resulted in formation of tri iodide. The interaction between the donor (RV) and HPA, H<sub>2</sub>CA acceptors was due to transfer of proton from acceptor to nitrogen atom of donor to make hydrogen bonding, where the interaction mode between RV and DDQ occurs through the migration of *n*- or  $\pi$ -electrons in RV to  $\pi^*$  in the DDQ. The obtained complexes are thermally stable. Physical parameters such as ( $K_{CT}$ ,  $\epsilon_{CT}$ ,  $\mu$ ,  $\Delta G$ ,  $I_D$ ,  $f$ ,  $E_{CT}$ ) and antibacterial activities have been estimated.

Finally, we could conclude that the interaction of Rebavirin (RV) as a donor with different acceptors proceeds in a molar ratio of 1:2 and 1:1 according to Scheme 1 as follows:



Scheme 1. Proposed CT-complexes of Rebavirin (RV) with different electron acceptors

## REFERENCES

- [1] DK Roy; A Saha; AK Mukherjee, *Spectrochim. Acta*, **2005**, A61, 2017.
- [2] ME El-Zaria, *Spectrochim. Acta*, **2008**, A69(1), 216–221.
- [3] F Gutmann; C Johnson; H Keyzer; J. Molnár. *Charge-Transfer Complexes in Biochemical Systems*. Marcel Dekker Inc., **1997**.
- [4] M Pandeewaran; KP Elango, *Spectrochim. Acta*, **2010**, A75(5), 1462–1469.
- [5] FP Flá; J Palou; R Valero; CD Hall; P Speers, *J. Chem. Soc., Perkin Transactions*, **1991**, 2(12), 1925–1932.
- [6] R Foster. *Organic Charge Transfer Complexes*. Academic Press, London, UK, **1969**.
- [7] A Korolkovas. *Essentials of Medical Chemistry*, chapter 3, John Wiley & Sons, New York, NY, USA, 2<sup>nd</sup> Edition, **1998**, Chapter 3.
- [8] AM Slifkin. *Charge-Transfer Interaction of Biomolecules*. Academic Press, New York, NY, USA, **1971**.
- [9] FM Abou Attia, *Farmaco*, **2000**, 55(11-12), 659–664.
- [10] J Carter; V Saunders. *Virology, Principles and Applications*. John Wiley & Sons, **2007**.
- [11] GL Davis; E Esteban-Mur; V Rustgi; J Hoefs; SC Gordon; C Trepo; ML Shiffman; S Zeuzem; A Craxi; JK Albrecht, *New Engl. J. Med.*, **1998**, 339, 1493.
- [12] JG McHutchison; SC Gordon; ER Schiff; ML Shiffman; WM Lee; VK Rutsgi; ZD Goodman; MH Ling; S Cort; JK Albrecht, *New Engl. J. Med.*, **1998**, 339, 1485.
- [13] FA Berden; W Kievit; LC Baak, *Neth J. Med.*, **2014**, 72 (8), 388–400.
- [14] E Cholongitas; GV Papatheodoridis, *Ann Gastroenterol*, 2014, 27(4), 331–337.
- [15] TT Tran; *Am. J. Manag. Care*, 2012, 18 (14 Suppl), S340–9.
- [16] A Dozal; H Keyzer; HK Kim; WW Wang, *Int. J. Antimicrob. Agent*, **2000**, 14, 261.
- [17] AM Ortega-Prieto; J Sheldon; A Grande-Pérez; H Tejero; J Gregori; J Quer; JI Esteban; E. Domingo; C Perales. *In Vartanian, Jean-Pierre. PLoS ONE*, **2013**, 8(8): e71039.
- [18] J Paeshuysse; K Dallmeier; J. Neyts, *Current Opinion in Virology*, **2011**, 1(6), 590–8.
- [19] Q Zhu; N Li; Q Han; P Zhang; C Yang; X Zeng; Y Chen; Y Lv; X Liu; Z Liu, *Antiviral Research*, **2013**, 98(3), 373–9.
- [20] AS Gaballa, *Indian J. Chem.*, **2005**, 44A, 1372.

- [21] AS Gaballa; C Wagner; EM Nour, SM Teleb; MAF Elmosallamy; GN Kaluderovic; H Schmidt; D Steinbon, *J. Mol. Struct.*, **2008**, 876, 301-308.
- [22] AS Gaballa, *J. Mol. Struct.*, **2013**, 1043, 91-102.
- [23] MM Ali; AS Gaballa; RA Haggam; NA El-Khososy; SM Teleb, *J. chem. Pharm. Research*, **2014**, 6(11), 570-580.
- [24] MM Ali; AS Gaballa; SM Teleb, *Russian J. of General Chem.*, **2015**, 85(2),xxx-xxx.
- [25] AS Gaballa; AS Amin, *Spectrochim. Acta*, **2015**, A145, 302-312.
- [26] DA Skoog. *Principle of Instrumental Analysis*. 3<sup>rd</sup> Edition, Saunder College Publishing, New York, **1985**, Chapter 7.
- [27] DJ Beecher; AC Wong, *Appl. Microbiol.*, **1994**, 60, 4614-4616.
- [28] National Committee for Clinical Laboratory Standards. *Methods for Antimicrobial Susceptibility Testing of Anaerobic Bacteria: Approved Standard M11 A3.NCCLS*, Wayne, PA, USA, **1993**.
- [29] AS Gaballa; SM Teleb; E Rusanov; D Steinborn, *J. Inorg. Chim. Acta*, **2004**, 357, 4144-4150.
- [30] EM Nour; LH Chen; J Laane, *J. Phys. Chem.*, **1986**, 90, 2841.
- [31] PH Svensson; L Kloo, *Chem. Rev.*, **2003**, 103(5), 1649-1684.
- [32] X Yua; RH Atalla, *Carbohydrate Research*, **2005**, 340, 981-988.
- [33] SY Al-Qaradawi; HS Bazzi; A Mostafa; EM Nour, *J. Mol. Struct.*, **2011**, 998, 126.
- [34] A El-Kourashy, *Spectrochim. Acta*, **1981**, A37, 399.
- [35] R Abou-Ettah; A El-Korashy, *J. Phys. Chem.*, **1972**, 76, 2405.
- [36] H Tsubomura, RP Lang, *J. Am. Chem. Soc.*, **1961**, 83, 2085.
- [37] R Rathore; SV Lindeman; JK Kochi, *J. Am. Chem. Soc.*, **1997**, 119, 9393.
- [38] G Aloisi; S Pignataro, *J. Chem. Soc., Faraday Trans.*, **1972**, 69 534.
- [39] G Briegleb, *Z. Angew. Chem.*, **1960**, 72, 401; G Briegleb, *Z. Angew. Chem.*, **1964**, 76, 326.
- [40] R Abu-Eittah; F Al-Sugeir, *Can. J. Chem.*, **1976**, 54, 3705.
- [41] MEM Hassouna; GA Zaki, *Int. J. Adv. Research*, **2014**, 2(4), 453-461.
- [42] KM Al-Ahmary; MM Habeeb; EA Al-Solmy, *J. Mol. Liqs.*, **2011**, 162, 129.
- [43] AS Al-Attas; MM Habeeb; DS Al-Raimi, *J. Mol. Struct.*, **2009**, 928, 158.
- [44] AA Adam, *Spectrochim. Acta*, **2013**, A104, 1.
- [45] AS Gaballa; SM Teleb; E Nour, *J. Mol. Struct.*, **2012**, 1024, 32-39.
- [46] SM Teleb; AS Gaballa, *Spectrochim. Acta*, **2005**, A62(1-3), 140-145.
- [47] FJ Muhtadi, *Anal. Profiles Drug Subst.*, **1984**, 13, 737.
- [48] DW Mayo; FA Miller; RW Hannah. *Course Notes on the Interpretation of Infrared and Raman Spectra*. John Wiley & Sons, **2003**.
- [49] B Stuart. *Infrared Spectroscopy: Fundamentals and Applications*. John Wiley & Sons, Ltd, **2004**.
- [50] SW Azeem; MA Khan; I Ahmad, *Pak. J. Pharm. Sci.*, **2005**, 18, 33.
- [51] J Šesták; P Šimon, Editors. *Thermal Analysis of Micro, Nano-and Non-Crystalline Materials*. Springer Science+Business Media Dordrecht, **2013**.